0254-6124/2021/41(5)-836–09 *Chin. J. Space Sci.* 空间科学学报

ZHAO Moxin, ZHANG Yunhua, DONG Xiao, LI Dong, YANG Jiefang. A novel ship wake detection algorithm based on WTHT and radon transform. *Chin. J. Space Sci.*, 2021, **41**(5): 836-844. DOI:10.11728/cjss2021.05.836

A Novel Ship Wake Detection Algorithm Based on WTHT and Radon Transform*

ZHAO Moxin[1,2] ZHANG Yunhua[1,2] DONG Xiao[1,2]

LI Dong[1,2] YANG Jiefang[1]

1(*Key Laboratory of Microwave Remote Sensing, National Space Science Center, Chinese Academy of Sciences, Beijing* 100190)

2(*University of Chinese Academy of Sciences, Beijing* 100049)

Abstract This paper proposes a novel ship wake detection algorithm based on the White Top-hat Transform (WTHT) and the Radon transform, which aims to improve the contrast between the ship wake and the background so as to improve the detection performance on Synthetic Aperture Radar (SAR) images. The proposed algorithm includes two major processes, and one is to improve the contrast and another one is to locate the ship wake. In high sea state conditions, the contrast of ship wake and background can be very low, which makes it difficult to detect. In the first step, the proposed contrast improvement algorithm is applied to improving the contrast which helps for improving the detection performance. An attribute filter based on edge detection result is adopted here. In the second step the contrast improved image is transformed into the Radon domain followed by peak extraction process to find the wake, the WTHT is used once more in this step. Finally, in the last step, the wake is overlapped on the original image. Experimental results on Tiangong-2 Interferometric Imaging Radar Altimeter (InIRA) images are presented and compared with that obtained by using the classical algorithm, and in this way, the better performance of our algorithm is demonstrated.

Key words White Top-hat Transform (WTHT), Radon transform, SAR image, Ship wake, Contrast improvement, InIRA

Classified index TN 959.74

0 Introduction

The oceans cover approximately 71 percent of the Earth's surface, and there are a lot of ships that voyage in the sea every time and every day, so effective regulation of ships is especially essential. In the past decades, spaceborne Synthetic Aperture Radar (SAR) has been widely used to detect and monitor ships[1−4], since SAR is capable of working all day long in all weather conditions. The automatic detection of ship targets has been researched for decades[2]. Indeed, the ships in SAR images usually exhibit bright spots for coarse resolution SARs, but there are several factors that may influence the detection results, such as the ship structure and material, the SAR resolution, and the sea state. For these reasons, ship targets sometimes are indiscernible or buried in the ocean background. Compared with ship targets in SAR images, ship wake has a much bigger size and remains for a long time, so it is much easier to detect. Moreover, some studies have confirmed that wakes can be used to estimate further information about the ship, *e.g.* the heading direction and velocity[3,4], and its detection has been continuous-

* Supported by National Key R&D Program of China (2016YFC1401004) along with China Manned Space Program
Received March 16, 2020. Revised January 10, 2021
E-mail: zhangyunhua@mirslab.cn

ly focused on[1,2,5,6]. It is well known that, if an image contains a straight line, its Radon transform will exhibit a peak (trough) if the line is brighter (darker) than the surroundings[7,8]. With this property, Radon transform and Hough transform, especially Radon transform, have been widely used in ship wake detection[4−6,9]. However, the Radon transform has several limitations[7], *e.g.*, the ship targets may cause false detection. To solve this problem, enhancing the Radon domain information is commonly practiced in two strategies, i.e. preprocessing the image before Radon transform or developing innovative algorithms to get the Radon domain[7,10,11].

In Ref. [10], Ai *et al.* proposed a Constant False Alarm Rate (CFAR) detection algorithm which combines the ship detection with ship wake detection using normalized Hough transform. In considering the interpolation operation needed in implementing the Radon transform, Courmontagne performed the Radon transform by using the stochastic matched interpolation-filtering method[7], which has shown good performance on canceling out the speckle noise. Copeland *et al.* proposed the localized Radon transform to overcome the global drawback of the Radon transform[11]. Wavelet plays an important role in this field, *e.g.*, Kuo *et al.* applied a wavelet correlator to extract ship wake and remove background noise before Radon transform[12]. In Ref. [13], Yang *et al.* used morphological dictionary learning to decompose texture component and ship wake component before Radon transform. In Ref. [1], sparse regularization was used to enhance the information in the Radon domain.

Among all the wake detection algorithms, the White Top-hat Transform (WTHT)[14−17] is seldom used to improve the contrast of images. In this paper, the modified WTHT is first used to enhance ship wake contrast and then the WTHT is used again for peak extraction in the Radon domain. For low contrast images, the algorithm performs particularly well.

Since the dark wake can be transformed into a bright wake by greyscale inversion, we focus on bright wakes in this paper. The detection process mainly contains two stages: one is to get the contrast improved, and the other one is to transform the contrast improved image into the Radon domain and extract peaks. In the contrast improvement part, the WTHT along with the edge detection is implemented, and after which, the ship wake becomes brighter while the background becomes darker. Then the contrast improved image is transformed into the Radon domain. By using WTHT again and finding the regional maximum in the Radon domain, the all possible peaks can be extracted, and according to which, the locations of ship wakes can be obtained. Experiment on real data is conducted with the results compared with that by classical algorithms, which validates our proposed algorithm very well.

The images used in this paper come from Tiangong-2 Interferometric Imaging Radar Altimeter (InIRA), which was blasted off with the Tiangong-2 Space Lab in 2016[18]. It is a VV polarization Ku-band interferometric radar and is also an interferometric synthetic aperture radar. Different from traditional SARs, the incidence angle range of Tiangong-2 InIRA is 1°∼8° much smaller than that used by SARs. Its original spatial resolutions are about 30 m in azimuth and about 30∼200 m in range.

1 Proposed Ship Wake Detection Algorithm

1.1 Algorithm Overview and Objective

The algorithm herein presented is pixel based and aims to improve the detectability of ship wakes in low resolution and low contrast images. It is well known that accurate wake detection result can benefit the subsequent estimation of the ship heading, ship velocity and ship location[3,4]. On this merit, our algorithm can promote the progress of fully automatic ship wake detection which is helpful for ship regulation.

Figure 1 shows the whole processing flow chart, where step 2 is the major step, which carries out the pixel-based contrast improvement process based on WTHT and edge detection. Different from the traditional WTHT which applies the same structuring element to the whole image, different structuring ele-

ments are used to each subwindow according to the result of the attribute filter. The attribute filter involves edge detection, and the details are described in section 1.3. After every pixel is processed, the Radon transform is used to locate the ship wake in step 3. In both step 2 and step 3, the WTHT is the core process. The classical wake detection algorithm contains only three steps: input image, Radon transform and peak detection, and label wake.

1.2 WTHT

1.2.1 Definition

Mathematical morphology is a theory widely used in image processing[14]. The basic grey scale morphological operations are erosion and dilation which are defined respectively as:

$$(F \ominus S)(x,y) = \min\{[F(x+x',y+y') - S(x',y')|(x',y') \in D_{\mathrm{s}}]\}, \quad (1)$$

$$(F \oplus S)(x,y) = \max\{[F(x-x',y-y') + S(x',y')|(x',y') \in D_{\mathrm{s}}]\}. \quad (2)$$

where F is the filtered image, S is the structuring element, D_{s} is the domain of S, "$\ominus$" denotes the erosion operator, and "$\oplus$" denotes the dilation operator. Erosion and dilation are similar to spatial correlation and convolution, respectively. The structuring element is similar to the mask in correlation or convolution and it can be any shape according to different specific situations. The common shapes include lines, squares, diamonds, and so on. For erosion, as Eq. (1) shown, the origin (denoted by "·" in Figure 2) of the structuring element is slidden to all pixel positions of F, and at every pixel location, the structuring element values are subtracted from the image pixel, and then get the minimum, which is the erosion result of the corresponding pixel. As for dilation, it is different from erosion, the structuring element should be rotated by 180° about its origin before sliding, the rotated structuring element values are then added to the image pixel, and get the maximum[14].

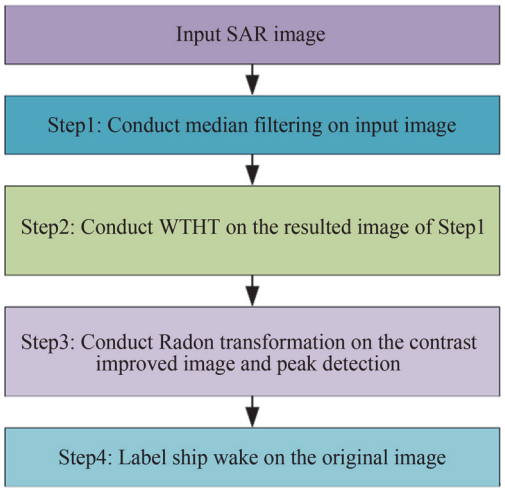


Fig. 1 Flow chart of the proposed algorithm

The WTHT involving erosion and dilation is defined as:

$$T_w(F,S) = F - [(F \ominus S) \oplus S]. \quad (3)$$

The operation of Eq. (3) is as follows. First, the image is eroded by S, then the eroded image is dilated by S, and finally, the dilated image is subtracted from the original image. The above WTHT has been widely used in image processing to extract shapes and homogenize backgrounds[15−17].

1.2.2 Linear Feature Enhancement Property

As it is known, the WTHT can remove objects smaller than the structuring elements[19]. Hence, if the structuring element is chosen as a flat linear structuring element with a specific direction, the WTHT can remove the same direction linear features which are smaller than the structuring element. Inspired by the refined Lee filter[19], it is supposed that the linear feature in an image can be divided into four categories, *i.e.*, 90°, 135°, 0°, and 45°, which are denoted by L_1, L_2, L_3, L_4[17], respectively. If an image area has a main linear feature L_m, $m = 1,2,3,4$, then it can be enhanced by removing the linear feature which is perpendicular to L_m. To achieve the goal, the WTHT is implemented by using a flat linear structuring element named L_m, whose direction is vertical to L_m and whose size is bigger than L_m. It means that the

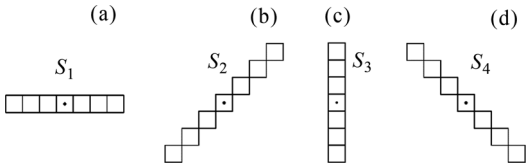


Fig. 2 Four structuring elements corresponding to 0°, 45°, 90° and 135°, respectively

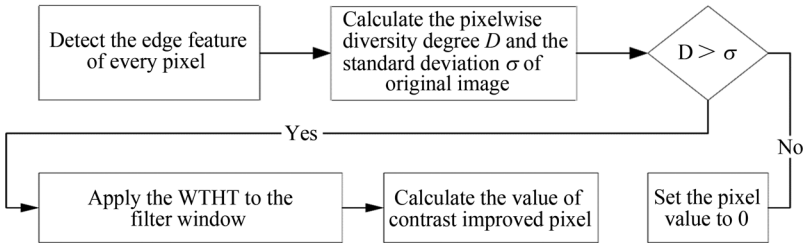


Fig. 3 Flow chart for pixelwise contrast improvement process

structuring elements can control the linear feature of the white top-hat transformed image. So if appropriate linear structuring elements are used in different windows, the linear feature of every window can be enhanced. Figure 2 shows the four structuring elements used in this work.

1.3 Contrast Improvement Process

Before the contrast improvement process is implemented, the Median filter is used to smooth the image. The contrast improvement process is pixelwise and based on the WTHT and edge detection. Figure 3 shows the flowchart of this operation.

1.3.1 Edge Detection

In order to determine whether the pixel belongs to the ship wake or not and get the orientation feature of the wake pixel, the edge operator is applied to a moving window whose center is the object pixel. However, as the process of extracting edge features in the refined Lee filter shown, if the edge operator is applied to the original moving window directly, the noise could pollute the edge detection result[19]. So, a 7×7 moving window is used to construct a group of 3×3 matrices named $\boldsymbol{W}$, which is then used to reduce the influence of noises as does in the Lee filter. A larger or smaller window can be constructed similarly if it is desired. A larger window cares more about the large structures while a smaller window cares more about the details. As shown in Figure 4, the center of a 7×7 window named N is the object pixel, which is divided into nine overlapped sub-windows. The new central pixel value of the constructed 3×3 window $\boldsymbol{W}$ equals the mean value of this sub-window. This operation allows some noises to cancel out, so the noise level can be lowered down. Eq. (4) gives the mathematical definition of $\boldsymbol{W}$,

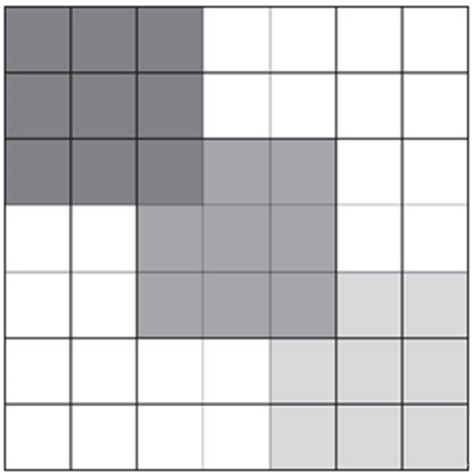


Fig. 4 Construction of the 3×3 matrix

$$\underset{\boldsymbol{T}_1}{\begin{bmatrix} -1 & 0 & 1 \\ -1 & 0 & 1 \\ -1 & 0 & 1 \end{bmatrix}} \quad \underset{\boldsymbol{T}_2}{\begin{bmatrix} 0 & 1 & 1 \\ -1 & 0 & 1 \\ -1 & -1 & 0 \end{bmatrix}} \quad \underset{\boldsymbol{T}_3}{\begin{bmatrix} 1 & 1 & 1 \\ 0 & 0 & 0 \\ -1 & -1 & -1 \end{bmatrix}} \quad \underset{\boldsymbol{T}_4}{\begin{bmatrix} 1 & 1 & 0 \\ 1 & 0 & -1 \\ 0 & -1 & -1 \end{bmatrix}}$$

Fig. 5 Four edge operators, denoted by $\boldsymbol{T}_1$, $\boldsymbol{T}_2$, $\boldsymbol{T}_3$, and $\boldsymbol{T}_4$, respectively

$$\boldsymbol{W}_{x,y} = \Big(\sum_{\substack{i=(2-x):(2x-1) \\ j=(2y-1):(2y+1)}} N_{i,j} \Big) \Big/ 3, \quad x = 1,2,3, \quad y = 1,2,3. \tag{4}$$

In the following, $\boldsymbol{W}$ is used along with four edge operators, *i.e.*, $\boldsymbol{T}_1$, $\boldsymbol{T}_2$, $\boldsymbol{T}_3$, $\boldsymbol{T}_4$, as shown in Figure 5, to get the orientation feature of the object pixel, from left to right, the edge operators are the vertical template, the 135° template, the horizontal template, and the 45° template, respectively. After multiplying the four edge operators with $\boldsymbol{W}$ element by element and then summing the products, four numbers, *i.e.*, N_1, N_2, N_3, N_4, can be gotten as follow:

$$N_1 = \mathrm{sum}[\mathrm{sum}(\boldsymbol{T}_1 .* \boldsymbol{W})], \tag{5}$$

$$N_2 = \mathrm{sum}[\mathrm{sum}(\boldsymbol{T}_2 .* \boldsymbol{W})], \quad (6)$$

$$N_3 = \mathrm{sum}[\mathrm{sum}(\boldsymbol{T}_3 .* \boldsymbol{W})], \quad (7)$$

$$N_4 = \mathrm{sum}[\mathrm{sum}(\boldsymbol{T}_4 .* \boldsymbol{W})]. \quad (8)$$

The ".∗" means multiplying arguments element-wise.

1.3.2 Wake Pixel Judgement

The above-obtained N_1, N_2, N_3 and N_4 are used to classify whether the object pixel belongs to the ship wake or not and get the orientation feature of the ship wake pixel. If the pixel belongs to the ship wake, then it should have significant direction characteristics, and the diversity degree of N_1, N_2, N_3 and N_4 will be large. The definition of diversity degree D is as follows, which indicates how different the four numbers are.

$$M = (N_1 + N_2 + N_3 + N_4)/4, \quad (9)$$

$$D = \big[(N_1 - M)^2 + (N_2 - M)^2 + (N_3 - M)^2 + (N_4 - M)^2\big]^{1/2}. \quad (10)$$

The larger the D, the more likely the object pixel belongs to the ship wake. Figure 6(a) presents a SAR image containing a ship wake from Tiangong-2 InIRA and Figure 6(b) shows the diversity degree image of Figure 6(a). It is clear to see from Figure 6 that the pixels belonging to the ship wake are more likely to have larger D values than the other pixels have. Meanwhile, it can be observed that the wake has two arms in the D image, and each of them may have two edges corresponding to the transition from background to wake and the transition from wake to the background. Fortunately, this dark stripe is usually much narrower than the bright edges, so they do not bring troubles for later operations. The standard deviation σ of the original image is taken as the threshold to distinguish ship wake pixel from background pixel. If $D > \sigma$, the pixel is classified as a ship wake pixel, otherwise if $D \leqslant \sigma$, the pixel is classified as a background pixel.

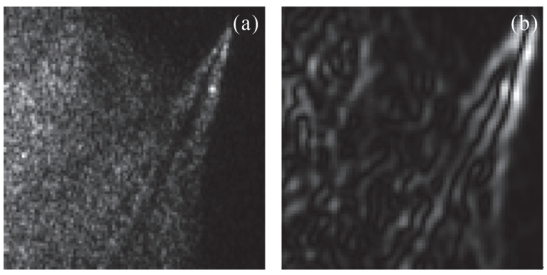


Fig. 6 Ship wake image and its diversity degree

If the pixel is classified as a background pixel, the corresponding pixel value of the contrast improved image is set to zero. If not, the linear orientation can be obtained according to N_1, N_2, N_3, and N_4. Then according to the linear orientation, an appropriate structuring element is chosen and the WTHT is applied to the window of appropriate orientation.

1.3.3 WTHT in Filter Window

For every pixel classified as a ship wake pixel, an appropriate structuring element and filter window should be chosen to implement the WTHT. If the maximum number is N_1, it means that the edge orientation is vertical. To enhance the vertical linear feature, the horizontal linear feature should be deleted. So, the horizontal structuring element of S_1 as shown in Figure 2 should be chosen. Similarly, if the maximum number is N_2, N_3 or N_4, then the structuring element of S_2, S_3 or S_4 should be chosen.

The filter window has the same direction as the structuring element has, and the center is the object pixel belonging to the ship wake. After applying the WTHT to a filter window, the filtered window can be obtained. The corresponding pixel value of the contrast improved image should be the central pixel value of the filtered window.

The size of the structuring element should be carefully chosen. If the size is too large, the effect of homogenizing background will be reduced, while if the size is too small, the linear feature of ship wakes will be destroyed[3]. Therefore, the wider the ship wake is, the larger the structuring element should be. To reduce unnecessary computation, the horizontal and vertical dimensions of the filter window should be smaller than the structuring element. Empirically, for Tiangong-2 images, the size of the structuring element is set to be 7, while the size of the filter window is 5×5. These sizes can ensure the line features are well reserved while the background well darkened at the same time.

1.4 Radon Transform

After every pixel is processed, the contrast can be im-

proved significantly. The Radon transform is then applied to the contrast improved image to detect line structures. The Radon transform, proposed by Johann Radon[8], is an integral transform along all possible straight lines in the image domain, which maps lines in the image domain into points in the Radon domain. Therefore, if there are ship wakes in the original image, there should be peaks in its Radon domain and the position of the maximum value in every peak area is related to the location of the ship wake in the image. The Radon transform of a continuous image is defined as:

$$r(\rho,\theta)=\iint_D F(x,y)\delta(\rho-x\cos\theta-y\sin\theta)\mathrm{d}x\mathrm{d}y, \quad (11)$$

where r is the Radon domain, ρ is the distance between the origin and the integral line, θ is the angle between the integral line's vertical line and the x-axis, D is the whole 2-D x-y Euclidean space, $F(x,y)$ is the grey value of (x,y), δ is the Dirac delta function. The classical ship wake detection algorithm does not have the process of contrast improvement, but directly applies the Radon transform to the original image.

For better extraction of peaks in the Radon domain, the Radon domain is first smoothed by a Gaussian filter, then the WTHT is implemented again by using a disk structuring element to the whole Radon domain to extract all possible peaks[20]. After that, the regional maxima can be easily located. In this fashion, several peak regions can be identified.

2 Results and Discussion

To evaluate the contrast improvement performance of the proposed algorithm, we conduct detection experiments on several Tiangong-2 InIRA images with low contrast.

Figure 7(a) shows the first experimental image, which contains a v-shaped bright ship wake. As one can see, the grey values of the left side are relatively greater than that of the right side, and for the ship wake, one arm is long but narrow, while the other arm is wide but short. Figure 7(e) and (f) show the Radon domain of Figure 7(a) presented in the image and in the graph, respectively, where the wake peaks are unconspicuous and cannot be distinguished from "peaks" caused by bright background pixels. Figure 7(d) shows the detection result directly from Figure 7(a), obviously, it is not correct. Figure 7(b) is the contrast improved image using the proposed algorithm, from which one can notice that the grey values of the background have been reduced and the linear feature is well preserved. The edge of the ship wake is sharper compared with the original image, which is good for highlighting the peaks in its Radon domain. Its Radon domain is shown in different forms in Figure 7(g) and (h), respectively. In Figure 7(g), the Radon domain is displayed as an image containing two clear peaks. Figure 7(h) graphs the Radon domain, from which one can easily get the two peaks as circled. The two peaks can be automatically detected as shown in Figure 7(i) which are corresponding to the two arms of the ship wake, and the final detection result is presented in Figure 7(c), as can be seen, the wake is very accurately detected and marked.

It should be addressed that if the peak extraction process is conducted on the original image transformed Radon domain directly, it would be hard to extract wake peaks. As shown in Figure 7(j), there are four peaks detected, and the peak 2 and 4 actually belong to one peak region because of the Radon transform ambiguity at 0° and 180°, while peak 1 and peak 3 are not real wake peaks because they are caused by the background.

Figure 8 and Figure 9 present another two results of experiments, named experiment 2 and experiment 3, respectively. In Figure 8(a), as can be seen, the ship wake also has two arms, but the contrast is quite low in the original image, and the ship wake is almost submerged in the clutter. Figure 8(e) shows the Radon domain of the original image, where the wake peaks are too ambiguous to extract. But from the image processed by the proposed algorithm, as shown in Figure 8(b), the contrast has been improved significantly, and its Radon domain with circled peak areas is shown in Figure 8(d). Figure 8(c) presents the detection result finally. In the case of Figure 9, an image containing a ship wake with three arms is processed. The bright clutter at the top left corner of

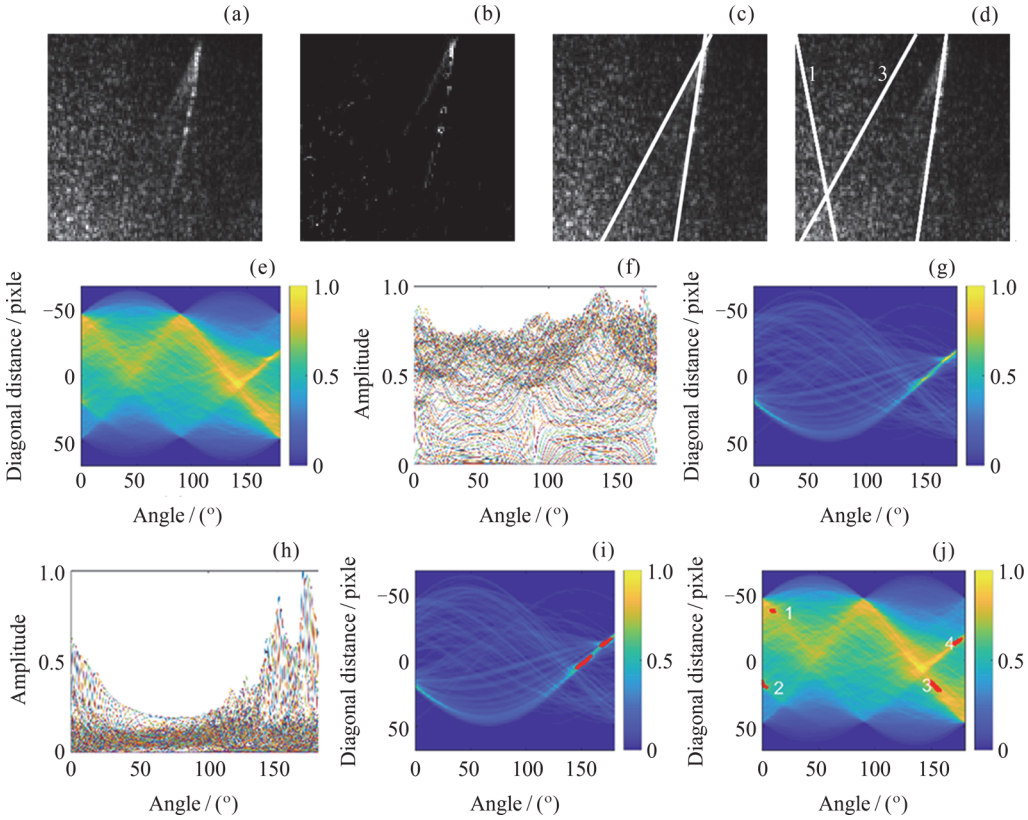


Fig. 7 Detection results of experiment 1, the color bar denotes the normalized amplitude in Radon domain. (a) Original image. (b) Contrast improved the image. (c) Detection result of (b). (d) Detection result of (a). (e) Radon domain of (a) is displayed as an image. (f) Radon domain of (a) is displayed as a graph. (g) Radon domain of (b) is displayed as an image. (h) Radon domain of (b) is displayed as a graph. (i) Peak detection result of (g). (j) Peak detection result of (e)

Table 1 RPVs for the original image and the contrast improved image

Experiment	RPV for the original image	RPV for the contrast improved image
1	0.0060	0.0310
2	0.0037	0.0099
3	0.0046	0.0223

Figure 9(a) is suppressed in Figure 9(b) where the contrast has been remarkably improved. The three arms are exactly detected as shown in Figure 9(c).

To quantitatively evaluate the effect of contrast improvement, the Ratios of the sum of the ship wake Peak area values of the Radon domain to the sum of all Radon domain Values (RPVs) for the above experiments are listed in Table 1 for comparison. Experiment 1 is based on the results of Figure 7 while experiment 2 and 3 are based on the results of Figure 8 and Figure 9, respectively. Table 1 clearly shows that the RPVs of the contrast improved images are higher than those of the corresponding original images. For example, for experiment 1, the RPV is improved about 5 times from 0.006 to 0.0310.

3 Conclusion

A novel ship wake detection algorithm based on the WTHT and the Radon transform has been proposed. The algorithm first improves the contrast between the ship wake and the background by using edge detec-

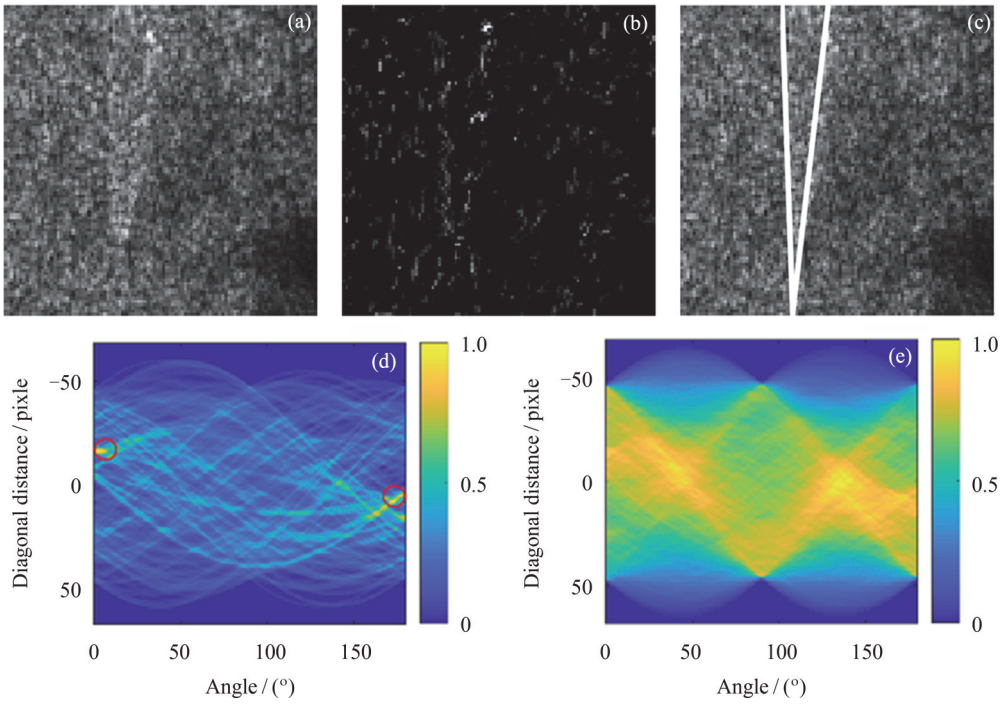


Fig. 8 Detection results of experiment 2, the color bar denotes the normalized amplitude in Radon domain. (a) Original image. (b) Contrast improved the image. (c) Detection result of (b). (d) Radon domain of (b) is displayed as an image with peak areas circled. (e) Radon domain of (a) is displayed as an image

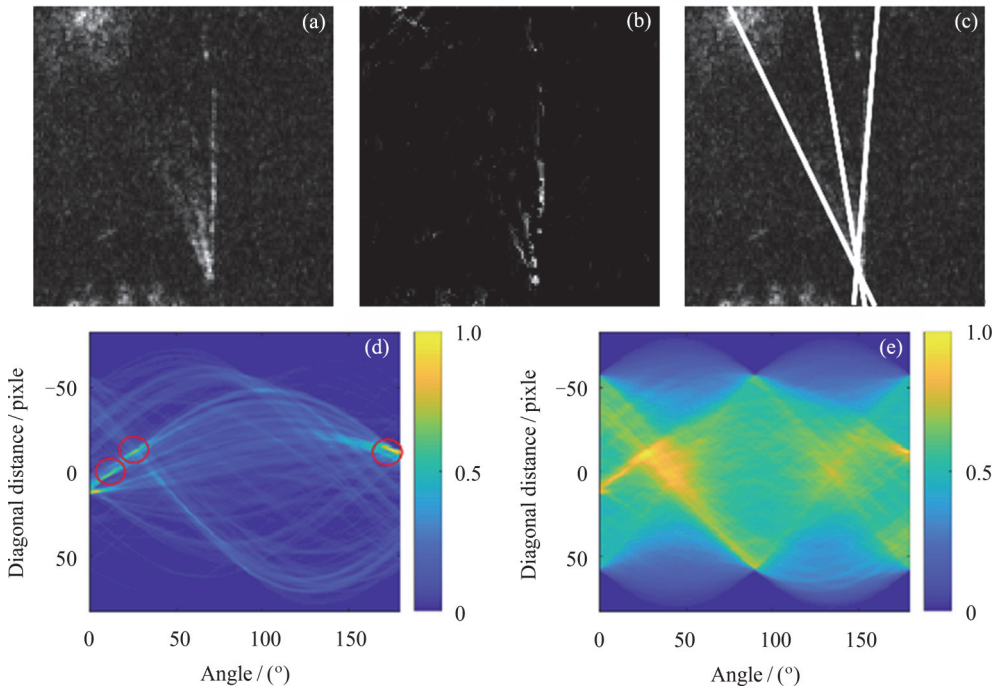


Fig. 9 Detection results of experiment 3, the color bar denotes the normalized amplitude in Radon domain. (a) Original image. (b) Contrast improved the image. (c) Detection result of (b). (d) Radon domain of (b) is displayed as an image with peak areas circled. (e) Radon domain of (a) is displayed as an image

tion and WTHT. Rather than applying the WTHT to the whole image using the same structuring element, the filter window and structuring element are chosen according to the wake pixel judgement result. The processing can darken the background and brighten ship wakes. Also, it can sharp the ship wake edges, which can highlight the peaks corresponding to ship wakes in the Radon domain. After the contrast is improved, the image is transformed into the Radon domain. Then we extract the peaks in the Radon domain by using the WTHT once more and detect the regional maxima.

Three experiments are conducted to process three different data sets by the proposed algorithm and by the classical algorithm, and the results show that our algorithm outperforms the classical algorithm. In the future, more experiments will be done as our algorithm continuously improves. How to distinguish different kinds of ship wakes is still an open problem to solve.

References

[1] KARAKUS O, RIZAEV I, ACHIM A. Ship wake detection in SAR images *via* sparse regularization [J]. *IEEE Trans. Geosci. Remote Sens.*, 2020, **58**(3): 1665-1677

[2] ELDHUSET K. An automatic ship and ship wake detection system for spaceborne SAR images in coastal regions [J]. *IEEE Trans. Geosci. Remote Sens.*, 1996, **34**(4): 1010-1019

[3] GRAZIANO M D, D'ERRICO M, RUFINO G. Wake component detection in X-band SAR images for ship heading and velocity estimation [J]. *Remote Sens.*, 2016, **8**(498): 1-15

[4] GRAZIANO M D, D'ERRICO M, RUFINO G. Ship heading and velocity analysis by wake detection in SAR images [J]. *Acta Astronaut.*, 2016, **128**: 72-82

[5] JIN Yaqiu, WANG Shiqing. An algorithm for ship wake detection from the SAR images using the Radon transform and morphological image processing [J]. *J. Syst. Eng. Elect.*, 2001, **12**(4): 7-12

[6] REY M T, TUNALEY J K, FOLINSBEE J T. Application of radon transform techniques to wake detection in Seasat-A SAR images [J]. *IEEE Trans. Geosci. Remote Sens.*, 1990, **28**(4): 553-560

[7] COURMONTAGNE P. An improvement of ship wake detection based on the radon transform [J]. *Signal Proc.*, 2005, **85**(8): 1634-1654

[8] RADON J. On the determination of functions from their integral values along certain manifolds [J]. *IEEE Trans. Med. Imag.*, 1986, **5**(4): 170-176

[9] BIONDI Filippo. Low-rank plus sparse decomposition and localized radon transform for ship-wake detection in synthetic aperture radar images [J]. *IEEE Geosci. Remote Sens. Lett.*, 2018, **15**(1): 117-121

[10] AI Jiaqiu, QI Xiangyang, YU Weidiong, *et al.* A novel ship wake CFAR detection algorithm based on SCR enhancement and normalized Hough transform [J]. *IEEE Geosci. Remote Sens. Lett.*, 2011, **8**(4): 681-685

[11] COPELAND A C, RAVICHANDRAN G, TRIVEDI M M. Localized Radon transform-based detection of ship wakes in SAR images [J]. *IEEE Trans. Geosci. Remote Sens.*, 1995, **33**(1): 35-45

[12] KUO Jinmin, CHEN K. The application of wavelets correlator for ship wake detection in SAR images [J]. *IEEE Trans. Geosci. Remote Sens.*, 2003, **41**(6): 1506-1511

[13] YANG Guozheng, YU Jing, XIAO Chuangbai, *et al.* Ship wake detection for SAR images with complex backgrounds based on morphological dictionary learning [C]//2016 IEEE International Conference on Acoustics, Speech and Signal Processing (ICASSP). Shanghai: IEEE, 2016: 1896-1900

[14] GONZALEZ R C, WOODS R E. Morphological Image Processing [M]. Digital Image Processing, 3rd ed. USA: Prentice-Hall, 2008: 649-709

[15] LI Yong, YONG Bin, WU Huayi, *et al.* Filtering airborne lidar data by modified white top-hat transform with directional edge constraints [J]. *Photogramm. Eng. Remote Sens.*, 2014, **80**(2): 133-141

[16] WANG Guoqing, WANG Jun, LI Ming, *et al.* Hand vein image enhancement based on multi-scale top-hat transform [J]. *Cybernet. Inform. Technol.*, 2016, **16**(2): 125-134

[17] BAI Xiangzhi, ZHOU Fugen, XUE Bindang. Multiple linear feature detection through top-hat transform by using multi linear structuring elements [J]. *Optik*, 2012, **123**(22): 2043-2049

[18] ZHANG Yunhua, DONG Xiao, SHI Xiaojin, *et al.* Demonstration of ocean target detection by Tiangong-2 interferometric imaging radar altimeter [C]//2018 22nd International Microwave and Radar Conference (MIKON). Poznan: IEEE, 2018: 261-264

[19] LEE J S. Refined filtering of image noise using local statistics [J]. *Comput. Vision, Graph. Image Proc.*, 1981, **15**: 380-389

[20] On-Line Source. Available online [OL]. [2020-03-01]. https://stackoverflow.com/questions/43852754/find-peak-regions-in-2d-data